Processing of the seven valine tRNAs in *Escherichia coli* involves novel features of RNase P

Ankit Agrawal[1], Bijoy K. Mohanty[2] and Sidney R. Kushner[1,2,*]

[1]Department of Microbiology, University of Georgia, Athens, GA 30602, USA and [2]Department of Genetics, University of Georgia, Athens, GA 30602, USA

ABSTRACT

Here we report that RNase P is required for the initial separation of all seven valine tRNAs from three distinct polycistronic transcripts (*valV valW*, *valU valX valY lysY* and *lysT valT lysW valZ lysY lysZ lysQ*). Particularly significant is the mechanism by which RNase P processes the *valU* and *lysT* polycistronic transcripts. Specifically, the enzyme initiates processing by first removing the Rho-independent transcription terminators from the primary *valU* and *lysT* transcripts. Subsequently, it proceeds in the 3′ → 5′ direction generating one pre-tRNA at a time. Based on the absolute requirement for RNase P processing of all three primary transcripts, inactivation of the enzyme leads to a >4-fold decrease in the levels of both type I and type II valine tRNAs. The ability of RNase P to initiate tRNA processing at the 3′ ends of long primary transcripts by endonucleolytically removing the Rho-independent transcription terminator represents a previously unidentified function for the enzyme, which is responsible for generating the mature 5' termini of all 86 *E. coli* tRNAs. RNase E only plays a very minor role in the processing of all three valine polycistronic transcripts.

INTRODUCTION

The *Escherichia coli* genome contains 86 transfer RNA (tRNA) genes that are organized as either monocistronic transcripts or complex operons, containing other tRNAs, messenger RNAs (mRNA) or ribosomal RNA (rRNA) genes (1,2). Every transcribed tRNA precursor requires subsequent processing at both ends to generate the mature species that will be charged by their cognate aminoacyl tRNA synthetases. In addition, tRNAs that are part of polycistronic transcripts require initial endonucleolytic cleavages to generate the pre-tRNAs that undergo further processing at their 5′ and 3′ termini. The generally accepted model involves endonucleolytic cleavages of polycistronic transcripts by RNase E to generate pre-tRNAs (3–5). Subsequently, the ribozyme RNase P endonucleolytically removes the extra nucleotides at the 5′ terminus, while the 3′ terminus is processed exonucleolytically by a combination of RNase T, RNase PH, RNase D, RNase BN, RNase II and PNPase (6,7).

E. coli RNase P is an essential enzyme consisting of the C5 protein (encoded by *rnpA*) and the catalytic M1 RNA (encoded by *rnpB*) subunits (8,9). Although the enzyme has been shown to be involved in the maturation of 4.5S RNA (a component of the essential signal recognition particle) (10), other small RNAs (11), and in the processing of a few polycistronic mRNAs (12,13), the removal of the extra nucleotides at the 5′ end of tRNAs by RNase P has been described as an essential function in the biogenesis of mature tRNA species that can subsequently be aminoacylated (14). However, recent reports suggest that some tRNAs with unprocessed 5′ ends can still be aminoacylated both *in vitro* and *in vivo* (15,16).

More importantly, it has recently been demonstrated that RNase P is required for the endonucleolytic separation of certain polycistronic tRNA transcripts such as *valV valW*, *leuQ leuP leuV* and *secG leuU* (15,17). Thus, it was hypothesized that the essential function of RNase P might be related to the complete absence of a particular tRNA that was dependent on the enzyme for initial separation from polycistronic transcripts. In such a scenario, loss of cell viability would result from the shortage of chargeable tRNAs due to immature 3′ ends rather than an inhibition of tRNA charging due to unprocessed 5′ ends.

Here we have examined the 86 tRNA genes in *E. coli in silico* to determine if perhaps all of the tRNA genes for one specific amino acid were initially processed by RNase P. Based on previous studies (3,7,15,17), many of the tRNAs including those for His, Leu, Pro, Trp, Arg, Asn, Met, Cys, Ala, Gln, Ser, Phe, Thr, Ile and Tyr were ruled out. However, both Val and Lys were possibilities, since we have already shown that the two of the seven valine tRNAs (*valV* and *valW*, isotype 2) require RNase P for their initial processing (17) and the processing of the six lysine tRNA genes has not been previously studied. In fact, one lysine tRNA was part of a polycistronic transcript including three valine tR-

---

*To whom correspondence should be addressed. Tel: +1 706 542 8000; Fax: +1 706 542 3910; Email: skushner@uga.edu

NAs (*valU valX valY lysV*), while the other five lysine tRNA genes were clustered together with two valine tRNAs (*lysT valT lysW valZ lysY lysZ lysQ*). However, it has been indicated that the *lysT* gene cluster is synthesized as four separate transcripts [18].

We now show that the *lysT* promoter drives the synthesis of a large polycistronic transcript that includes all seven tRNAs. More importantly, all seven valine tRNAs require RNase P for their initial processing. Interestingly, RNase P processing occurs in the 3'→ 5' direction, generating one pre-tRNA at a time. Thus, functional valine tRNAs, either isotype 1 or 2, are no longer generated, from their primary transcripts upon inactivation of RNase P, leading to a >4-fold drop in the levels of mature valine tRNAs. However, exogenous expression of both valine tRNA isotypes processed independently of RNase P did not complement an *rnpA49* mutant at the non-permissive temperature. We also show that the 3' → 5' exonuclease, RNase PH, plays a major role in the 3′ end maturation of type I valine isotype tRNAs.

MATERIALS AND METHODS

Bacterial strains

All the *E. coli* strains used in this study were derivatives of MG1693 (*thyA715 rph-1*) and are listed in Table 1. The *rne-1* and *rnpA49* mutations, encoding temperature-sensitive RNase E and RNase P enzymes, respectively, do not support cell viability at either 42 or 44°C and have been previously described [19,20]. A P1 phage lysate grown on SK2525 (*rnpA49 rph-1*) was used to transduce both SK10153 (*thyA715*) and SK9797 (*rne-1 rnzΔ500 rph-1*) to generate SK10521 and SK10300, respectively. SK5166 (*rnpA49 rph-1*) was transduced with a P1 lysate grown on SK4455 (*rnc-14 rph-1*) to construct SK10525. A P1 lysate grown on SK3170 (*rnlA2 rph-1*) was used to transduce SK2534 (*rne-1 rnpA49 rph-1*) to construct SK10523. SK10460 [*rneΔ1018 rnpA49*/pDH28(*rng-219*/Km^R)] was constructed by the plasmid displacement from SK2539 [*rneΔ1018 rnpA49*/pMOK15(*rneΔ610*/Cm^R)] (Ow and Kushner, unpublished results).

Plasmid constructions

The plasmids pAAK11 (*valU*^+/ Cm^R), pAAK15 (*argX*^+/Cm^R) and pAAK17 (*rnpB*^+/Cm^R) all contain the p15A origin of DNA replication (15–20 copies/cell) and express either *valU, argX* or the M1 RNA (*rnpB*), respectively, under the control of the *lac* promoter. Plasmid pAAK13 (*valW*^+ /Sm^R) is a 6–8 copy plasmid with a pSC101 origin of DNA replication expressing *valW* under the control of the *lac* promoter. A PCR (polymerase chain reaction) fragment containing a *lac* promoter followed by a gene of interest (either *valU, valW, argX or rnpB*) and a Rho-independent transcription terminator [derived from *leuU*, [15]] was generated employing an overlapping PCR technique using Phusion® High-Fidelity DNA Polymerase (NEB). The resulting PCR products were cloned into the BamHI/HindIII sites of either pBMK11 [21] to construct pAAK11 (*valU*^+/ Cm^R), pAAK15 (*argX*^+/Cm^R) and pAAK17 (*rnpB*^+/Cm^R) or pMS421 [22] to construct pAAK13 (*valW*^+/Sm^R).

All the plasmid constructions were confirmed by DNA sequencing of the cloned fragments (Eurofins MWG Operon). In addition, Northern analysis was used to confirm that the isopropyl-β-D-1-thiogalactopyranoside (IPTG) induction of plasmids pAAK11, pAAK13, pAAK15 and pAAK17 led to increased intracellular levels of tRNA^Val1, tRNA^Val2, tRNA^Arg and M1 RNA, respectively. Plasmid transformations were carried out as described previously [23].

Bacterial strains were typically grown with shaking in Luria broth [24] supplemented with thymine (50 µg/ml). When appropriate, the medium also contained tetracycline (20 µg/ml), kanamycin (25 µg/ml), chloramphenicol (20 µg/ml) or streptomycin (20 µg/ml). Culture growth was monitored using a Klett-Summerson Colorimeter (No.42 Green filter). For temperature-sensitive mutant strains, cultures were initially grown at 30°C until they reached 50 Klett units above background and then shifted to 44°C, unless noted otherwise. All the cultures were maintained in exponential growth by periodic dilutions with pre-warmed medium. To collect samples for RNA extraction, RNase P (*rnpA49* allele) and RNase E (*rne-1* allele) mutant strains were shifted to 44°C for 1 and 2 h, respectively. The wild-type control strains were also shifted to 44°C for 1 h.

Isolation of total RNA

Total RNA for steady-state analysis was extracted using the method described by Mohanty *et al.* [25], with the following modifications. Cell pellets from 3.5 ml of cells were resuspended in 510 µl of Lysis buffer. After lysis, 71 µl of 20 mM acetic acid were added. Following resuspension in 1 ml of 2 M LiCl, each sample was centrifuged at 16 000 x g for 10 min. The resulting pellets were washed with 500 µl of chilled 70% ethanol, followed by centrifugation at 10 000 x g for 10 min. The supernatants were removed and the pellets were spun again at 10 000 x g for 1 min to remove any residual ethanol.

Total RNA for half-life analyses was extracted using the RNA*snap*^TM method [26]. Rifampicin (500 µg/ml) and nalidixic acid (20 µg/ml) were added to the cell cultures at 50 Klett units above background and the samples for 0-min time-point were collected after 70 s [25]. All RNA samples were quantified using a NanoDrop (Model 2000c; Thermo Scientific) apparatus. In addition, 500 ng of each RNA sample was separated on a 1% agarose gel and visualized by ethidium bromide staining to check for RNA integrity and to ensure equal loading.

Northern analysis and determination of *in vivo* aminoacylation levels

Northern analysis was carried out as described by Mohanty and Kushner [17]. Briefly, 12 µg of total RNA from each strain were separated on either 6 or 8% polyacrylamide gels containing 8.3 M urea in TBE buffer or 1.2% agarose gels and were subsequently transferred on to a positively charged nylon membrane (Nytran^TM SPC, Whatman^TM). ^32P-labeled DNA oligonucleotides were used as probes. The blots were scanned with a PhosphorImager

Table 1. List of bacterial strains and plasmids used in this study

Strains	Genotype	Reference/source
MG1693	*rph-1 thyA715*	*E. coli* Genetic Stock Center
SK2525	*rnpA49 rph-1 thyA715 rbsD296::*Tn*10* Tc^R	(4)
SK2534	*rne-1 rnpA49 rph-1 thyA715 rbsD296::*Tn*10* Tc^R	(4)
SK2549	*rne-1 rnpA49 rng::cat rph-1 thyA715 rbsD296::*Tn*10* Cm^R Tc^R	(43)
SK3170	*rnlA2::kan rph-1 thyA715* Km^R	Perwez & Kushner (unpublished results)
SK4455	*rnc-14 rph-1 thyA715* Tc^R	(44)
SK4484	*rne-1 rnpA49 rng::cat rnzΔ500::apr rnlA2::kan rph-1 rbsD296::*Tn*10* Cm^R Km^R Apr^R Tc^R	Maples and Kushner (unpublished results)
SK4668	*rne-1 rnpA49 rnb-500 pnp-7 rph-1 thyA715 rbsD296::*Tn*10* Tc^R	Maples and Kushner (unpublished results)
SK5166	*rnpA49 rph-1 thyA715 rbsD3163::*Tn*10::kan* Km^R	Stead & Kushner (unpublished results)
SK5374	*ΔybeY::cat rnpA49 rph-1 thyA715 rbsD296::*Tn*10* Cm^R Tc^R	Stead & Kushner (unpublished results)
SK5665	*rne-1 rph-1 thyA715*	(45)
SK5704	*rne-1 pnp-7 rnb-500 rph-1 thyA715*	(45)
SK9797	*rne-1 rph-1 rnzΔ500::kan thyA715* Km^R	(46)
SK10153	*thyA715*	(28)
SK10300	*rne-1 rnpA49 rnzΔ500::kan rph-1 thyA715 rbsD296::*Tn*10* Tc^R Km^R	This study
SK10451	*rnpA49 pnp-7 rnb-500 rph-1 thyA715 rbsD296::*Tn*10* Tc^R	(17)
SK10460	*Δrne-1018::bla*/pDHK28(*rng-219*/Km^R) *rnpA49 rph-1 thyA715 rbsD296::*Tn*10* Sm^R/Sp^R Ap^R Km^R Tc^R	This study
SK10523	*rne-1 rnpA49 rnlA2::kan rph-1 thyA715 rbsD296::*Tn*10* Tc^R Km^R	This study
SK10525	*rnc-14 rnpA49 rph-1 thyA715 rbsD296::*Tn*10* Tc^R Km^R	This study
SK10530	*rnpA49 rph-1 thyA715 rbsD296::*Tn*10* Tc^R/pAAK11	This study
SK10531	*rnpA49 thyA715 rbsD296::*Tn*10* Tc^R/pAAK11	This study
SK10533	*rnpA49 rph-1 thyA715 rbsD296::*Tn*10* Tc^R/pAAK13	This study
SK10534	*rnpA49 thyA715 rbsD296::*Tn*10* Tc^R/pAAK13	This study
SK10537	*rnpA49 rph-1 thyA715 rbsD296::*Tn*10* Tc^R /pAAK15	This study
SK10538	*rnpA49 thyA715 rbsD296::*Tn*10* Tc^R/pAAK15	This study
SK10539	*rnpA49 rph-1 thyA715 rbsD296::*Tn*10* Tc^R/pAAK17	This study
SK10540	*rnpA49 thyA715 rbsD296::*Tn*10* Tc^R/pAAK17	This study
SK10541	*rnpA49 rph-1 thyA715 rbsD296::*Tn*10* Tc^R/pAAK11 pAAK13	This study
SK10542	*rnpA49 thyA715 rbsD296::*Tn*10* Tc^R/pAAK11 pAAK13	This study
Plasmids		
pMS421	*lacI^{q+}*, Sm^R	(22)
pBMK11	*pcnB$^+$*, Cm^R	(21)
pAAK11	pBMK11, *valU$^+$*,Cm^R	This study
pAAK13	pMS421, *valW$^+$*,Sm^R	This study
pAAK15	pBMK11, *argX$^+$*,Cm^R	This study
pAAK17	pBMK11, *rnpB$^+$*,Cm^R	This study
pMOK15	*rneΔ610* Cm^R	(47)
pDHK28	*rng-219* Km^R	(32)

(Storm^{TM} 840; GE Healthcare). Each membrane was often probed with different probes after stripping as previously described (25). Band intensities were determined using ImageQuant TL 5.2 software (GE Healthcare). The percentage of tRNA aminoacylation level was determined as previously described (27,28).

Reverse transcription-polymerase chain reaction (RT-PCR) cloning and sequencing of 5′ → 3′ ligated transcripts

The 5′ and 3′ ends of various processing intermediates derived from the *valU* and *lysT* polycistronic transcripts were identified by cloning and sequencing RT-PCR products obtained from 5′ → 3′ end-ligated circular RNAs using the method described by Mohanty and Kushner (15,28,29). In brief, 3 μg of total RNA from *rph-1, rnpA49 rph-1* and *rne-1 rnpA49 rph-1* strains were initially treated with tobacco acid pyrophosphatase (Epicentre Technologies) to convert any 5′ triphosphates to phosphomonoesters in order to facilitate the self-ligation step. The dephosphorylated RNAs were self-ligated using T4 RNA ligase (NEB) and were subsequently reverse transcribed followed by PCR amplification using several pairs of gene-specific primers.

Primers and probes

The nucleotide sequences of all primers and probes used in this study are shown in Supplementary Table S1 (Supplementary Material). Table S1 RESULTS

Processing of the *valU* polycistronic transcript is completely dependent on RNase P

The seven valine tRNAs in the *E. coli* genome are organized into three separate gene clusters, *valV valW* (17), the *valU* and *lysT* operons (Figures 1A and 2A). The initial separation of the *valV valW* transcript, containing two copies of valine isotype 2, has been shown to be completely dependent on RNase P cleavages at the mature 5′ termini of both tRNAs (17). The remaining five valine tRNAs, belong to the valine isotype 1. Interestingly, the intergenic spacer regions between *valY* and *lysV* (CUUC)*, valT* and *lysW* (CC) and *valZ* and *lysY* (CUC) (Figures 1A and 2A) were very similar to the UCCU spacer between *valV* and *valW*. This observation suggested that RNase P might be involved in the initial processing of additional valine tRNAs, since these short spacer regions are not canonical RNase E cleavage sites (30,31).

Accordingly, we examined the processing of the *valU* operon in the *rph-1*, *rne-1 rph-1*, *rnpA49 rph-1* and *rne-1 rnpA49 rph-1* isogenic strains by Northern analysis using operon-specific oligonucleotide probes (Figure 1A). Since all five isotype I valine tRNAs have identical sequences, we
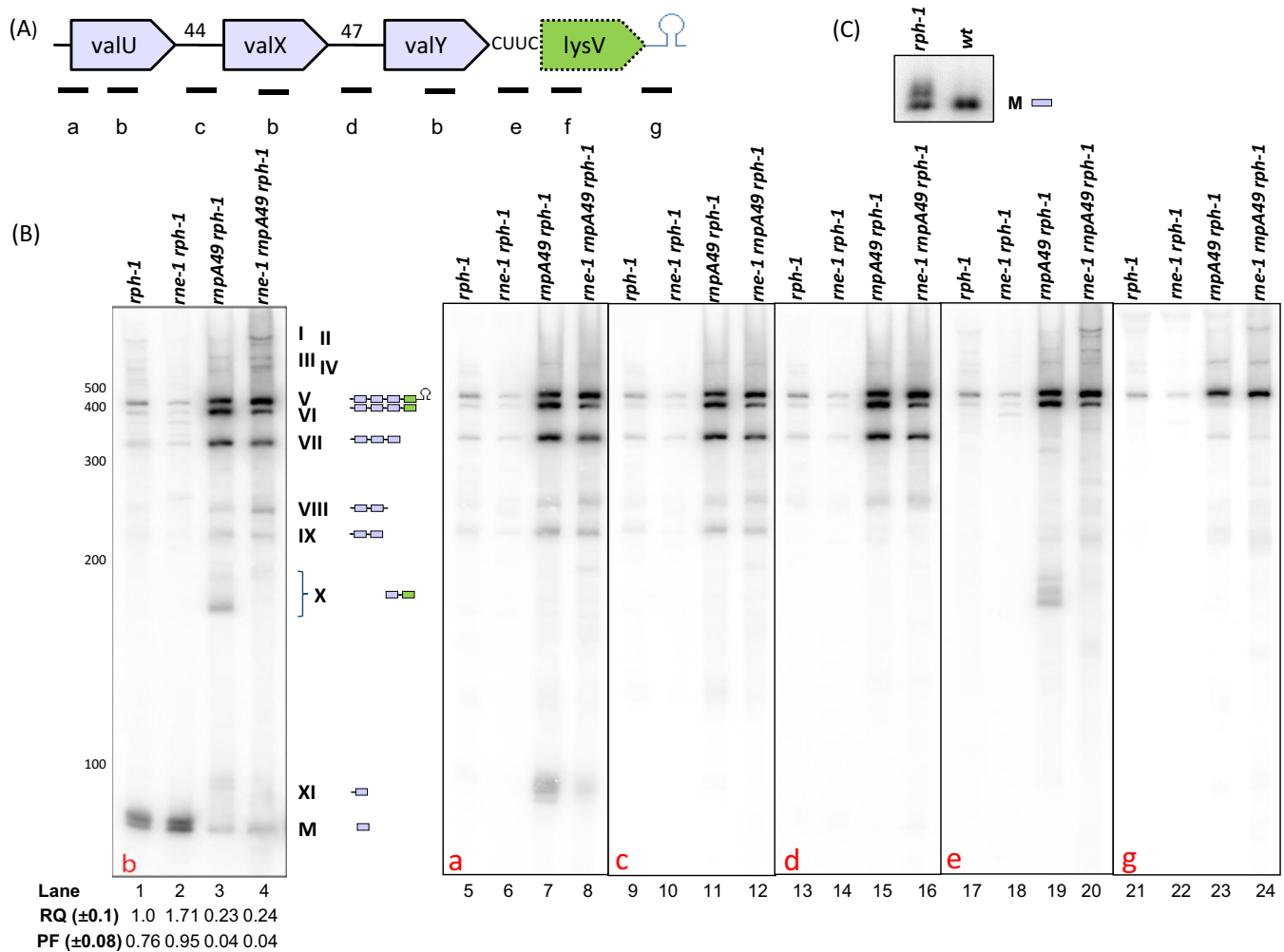
Figure 1. Analysis of *valU* operon processing. (**A**) Schematic diagram of the *valU* operon (not drawn to scale). Relative positions of the oligonucleotide probes (a: valU-UP, b: valUXYTZ, c: valU-X, d: valX-Y, e: valY-lysV, f: lysmature, g:lysV-TER) used in Northern analyses are shown. Probe sequences are listed in Supplementary Table S1 (Supplementary Materials). Numbers indicate the length of the intergenic spacers. (**B**) Northern analysis of *valU* operon. The specific oligonucleotide probe used for each blot is indicated in the bottom left corner of each blot. The genotypes of the strains used are listed on the top of each autoradiogram. The RNA molecular size standards (nucleotides) (Fermentas) are shown to the left of the first image. The numerical designations of the different species along with their graphical structures are shown to the right of the first blot. Relative quantity (RQ) of mature tRNA^{Val} (M) in various genetic backgrounds was calculated by setting a level of one in the *rph-1* strain. Processed fraction (PF) represents the fraction of mature tRNA relative to the total amount of processed and unprocessed species of that tRNA. Each value represents the average of at least three independent determinations. (**C**) Analysis of the role of RNase PH in the final maturation of the five valine type I tRNAs.

first probed with an oligonucleotide that was complementary to the mature valine type I coding sequence (probe b, Figure 1A). No significant differences in processing intermediates were observed between the *rph-1* and *rne-1 rph-1* strains (Figure 1B, lanes 1–2). The most prominent species were the mature tRNA (M) and a slightly larger band. This larger band was due to the RNase PH deficiency (*rph*-1) in all the strains resulting in unprocessed 3′ ends (See below). There were also three high molecular weight species (V, VI and VII) that were weakly visible (lanes 1, 2).

The intensity of species V, VI and VII increased dramatically in the absence of RNase P (*rnpA49 rph-1*) along with an almost 4-fold decrease in the amount of the mature species (M) (lane 3). In addition, new species (VIII, IX and X) appeared in the absence of RNase P. When both

RNase P and RNase E (*rne-1 rnpA49 rph-1*) were inactivated, species X disappeared along with slightly increased intensities of species V and VIII and small decreases in the levels of species VI and VII (lane 4), suggesting a very minor role for RNase E in the absence of RNase P. The level of mature species (M) remained unchanged compared to the *rnpA49 rph-1* double mutant. In fact, the processed fraction (PF) for the mature tRNA^{Val1} decreased from 0.76 and 0.95 in the *rph-1* and *rne-1 rph-1* strains, respectively, to 0.04 in the *rnpA49 rph-1* and *rne-1 rnpA49 rph-1* strains (lanes 1–4).

The composition of all the various processing intermediates seen in Figure 1B (lanes 1–4) was subsequently determined by probing the blot with oligonucleotides that were complementary to various regions of the operon (Figure 1A). For example, probe a (complementary to the up-
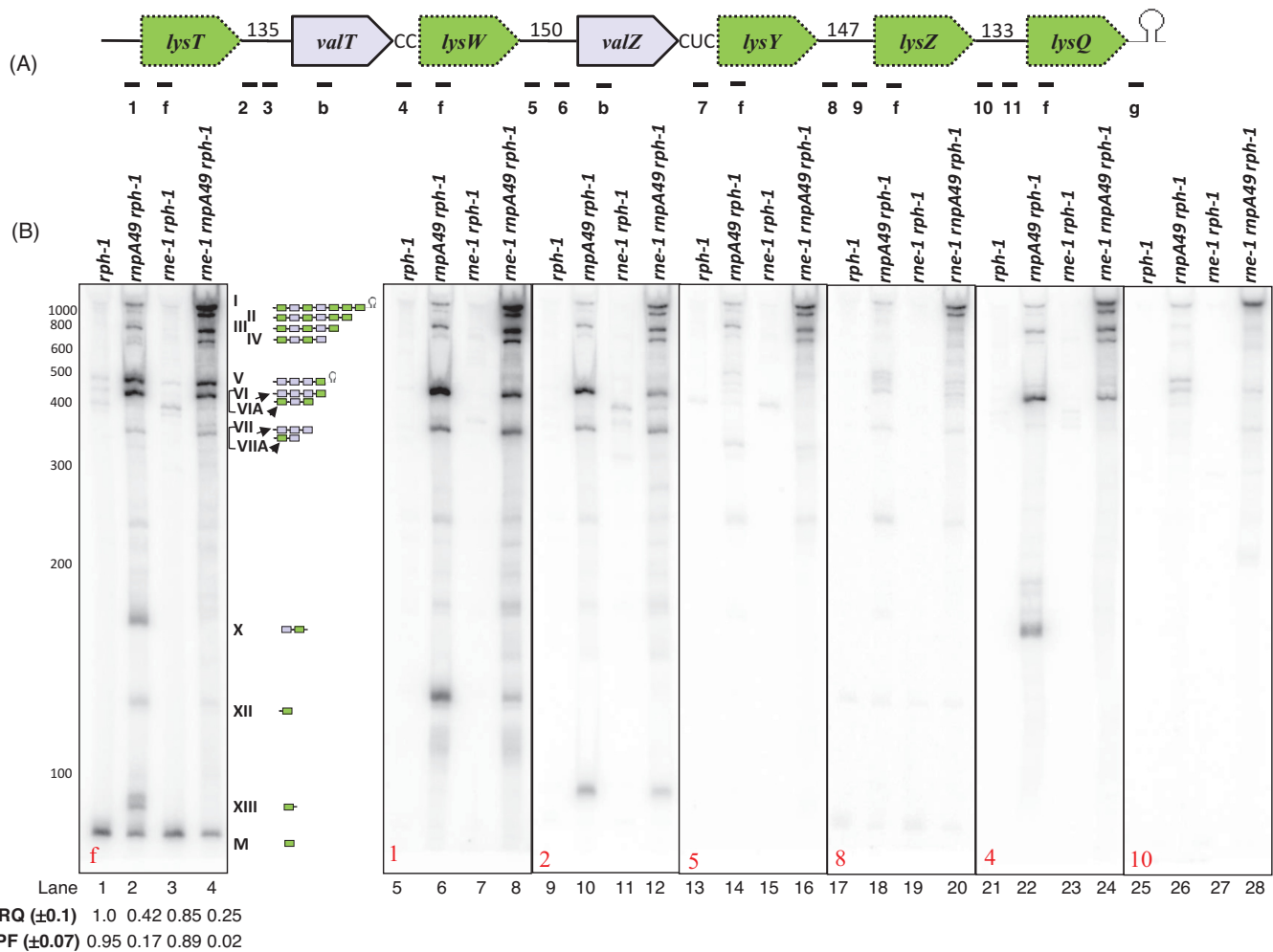
Figure 2. Analysis of the *lysT* operon processing. (**A**) Schematic diagram of the operon (not drawn to scale). Relative positions of the oligonucleotide probes (1: lysT-UP, f: lysmature, 2: lysT-valT1, 3: lysT-valT3, b: valUXYTZ, 4: valT-lysW, 5: lysW-valZ1, 6: valZ-UP2, 7: valZ-lysY, 8: lysY-lysZ1, 9: lysY-lysZ2, 10: lysZ-lysQ1, 11: lysZ-lysQ2, g: lysV-TER). Probe sequences are listed in Supplementary Table S1 (Supplementary Materials). Numbers indicate the length of the intergenic spacers. (**B**) Northern analysis of *lysT* operon. The specific oligonucleotide probe used in each blot is indicated in the bottom left corner of the blot. The genotypes of the strains used are indicated on the top of the each autoradiogram. The RNA molecular size standards (nucleotides) (Fermentas) are shown to the left of the first blot. The numerical designations of the different species along with their graphical structures are shown to the right of the blot. Bands VI and VII arise from the *valU* operon and comigrate with bands VIA and VIIA, respectively. Two independent Northern blots were run (one was probed with f, 1, 2, 5 and 8; second was probed with 4 and 10). The RQ and PF values were calculated as described in the legend to Figure 1.

stream region of *valU*) hybridized to all the processing intermediates (species V–IX, XI) with the exception of species X (lanes 5–8). In contrast, probe g (complementary to the Rho-independent transcription terminator, Figure 1A) only hybridized to species V (lanes 21–24) demonstrating that it was the full-length *valU* operon transcript (predicted size ~438 nt).

In addition, probes c, d and e hybridized to species V and VI (lanes 9–20). Since species VI also hybridized to probe a (lanes 5–8), but not to probe g (lanes 21–24), it was identified as the complete transcript minus the Rho-independent transcription terminator. Our data also suggested that the Rho-independent transcription terminator associated with species V was removed primarily by RNase P, because its level increased significantly in the *rnpA49 rph-1* strain compared to the *rne-1 rph-1* mutant (lanes 2, 3).

Probe e, which was complementary to the intergenic region between *valY* and *lysV* (Figure 1A), did not hybridize to either mature tRNA[Val] or tRNA[Lys] and also did not hybridize to species VII (Figure 1B, lanes 17–20). However, species VII was detected with probe d (lanes 13–16), indicating that it arose from a cleavage between *valY* and *lysV* tRNAs. In contrast, species VIII appeared to arise from a cleavage downstream of *valX*. The multiple bands labeled as species X were observed with probes b and e in the *rnpA49 rph-1* strain (lanes 3, 19), but disappeared in the *rne-1 rnpA49 rph-1* strain (lanes 4, 20). This result suggested that this group of processing intermediates containing valine coding sequences arose from occasional RNase E cleavages at different sites within the *valU* operon transcript in the *rnpA49 rph-1* strain.

Species XI was detected by probes b and a in the *rnpA49 rph-1* (lanes 3, 7), but with reduced intensity in the *rne-1 rnpA49 rph-1* strain (lanes 4, 8). However, this band was not detected with probe c (complementary to the intergenic region between *valU* and *valX*), even in the *rnpA49 rph-1* strain (lane 11), indicating that in the absence of RNase P, RNase E cleaved inefficiently in the intergenic region between *valU* and *valX*, resulting in a fragment containing *valU* with the 5′ leader sequence and perhaps some portion of the intergenic region at its 3′ end.

The detection of bands I-IV with probes b, e and g (Figure 1B, lanes 4, 20, 24) was initially surprising, since their sizes were much larger than the full-length *valU* polycistronic transcript. However, upon examining the sequences of the *valU* operon and *lysT* gene cluster (18), we realized that the intergenic region between *valY* and *lysV* (CUUC, Figure 1A) was similar to the intergenic regions between *valT* and *lysW* (CC, Figure 2A) and *valZ* and *lysY* (CUC, Figure 2A). Since all the five valine tRNAs and the six lysine tRNAs present in the *valU* operon and *lysT* gene cluster are identical to each other, respectively, we hypothesized that probes b and e (Figure 1A) were likely hybridizing to RNA fragments originating from both the *valU* operon and the *lysT* gene cluster. Additionally, we observed that the Rho-independent transcription terminators downstream of the *lysV* and *lysQ* genes were identical in sequence (data not shown). Thus, the large species detected with probes b, e and g (lanes 4, 20, 24) probably originated from transcripts of the *lysT* gene cluster (see below).

RNase PH is required for the final 3′ end maturation of the valine type 1 tRNAs

It should be noted that our experiments were carried out in a parental strain (MG1693) that was defective in RNase PH (*rph-1*). Sequence analysis of 5′ → 3′ ligated tRNAs from *rph-1* strains identified *val* tRNAs that had either one or two extra nucleotides downstream of the CCA determinant (data not shown). These results were consistent with the species that was slightly larger than the mature valine tRNA that was observed in the *rph-1* and *rne-1 rph-1* strains (Figure 1B, lanes 1, 2). In fact, the larger species disappeared in SK10153 an isogenic *rph*⁺ derivative of MG1693 (Figure 1C).

The *lysT* gene cluster is transcribed as a polycistronic transcript

Based on our observations with probes b, e and g (Figure 1B), we hypothesized that the larger species (I-IV) were derived from the *lysT* gene cluster, even though it is indicated in the EcoCyc database that the seven genes are part of four separate transcripts (18). If all seven tRNAs in the *lysT* gene cluster were synthesized as a polycistronic transcript, a full-length species of over 1100 nt would be generated. In fact, a species greater than 1100 nt in length (I) was observed in the *rnpA49 rph-1* and *rne-1 rnpA49 rph-1* strains (Figure 2B, lanes 2, 4) along with multiple lower molecular weight species (II, III, IV, V, VI, VIA, VII, VIIA, X, XII, XIII and M). However, only species I hybridized to both probe 1 (Figure 2A and B, lanes 6, 8) and probe g (Figures 1A and 2B, lane 24), demonstrating that it constituted

the full-length *lysT* transcript. The larger species (I-IV) were barely visible in the *rph-1* and *rne-1 rph-1* strains (Figure 2B, lanes 1, 3), suggesting a very minimal role for RNase E in processing the *lysT* transcript if RNase P were present.

Processing of the *lysT* polycistronic operon requires RNase P but is stimulated by RNase E

Unlike what was seen with the analysis of the *valU* operon, there was a single mature lysine tRNA species (M) in both the *rph-1* and *rne-1 rph-1* strains and surprisingly few other processing intermediates (Figure 2B, lanes 1, 3). In contrast, the amount of the mature tRNA^{Lys} species (M) was significantly reduced in the *rnpA49 rph-1* and *rne-1 rnpA49 rph-1* mutants (lanes 2, 4) along with a concomitant increase in larger species (I-V, VIA, VIIA, X, XII and XIII). In fact, the PF of mature tRNA^{Lys} decreased from 0.95 and 0.89 in the *rph-1* and *rne-1 rph-1* strains to 0.17 and 0.02 in the *rnpA49 rph-1* and *rne-1 rnpA49 rph-1* mutants, respectively.

To ascertain the composition of the larger species (I-IV), we probed the blot with oligonucleotides that were complementary to the 5′ leader region (Figure 2A, probe 1) as well as intergenic regions between *lysT* and *valT* (Figure 2A, probes 2, 3), *lysW* and *valZ* (probes 5, 6), *lysY* and *lysZ* (probes 8, 9), and *lysZ* and *lysQ* (probes 10, 11). With probes 10 and 11, species I, but not species II-IV, was observed in both *rnpA49 rph-1* and *rne-1 rnpA49 rph-1* strains (lanes 25–28; data not shown). It should be noted that the additional bands present in Figure 2B, lanes 26 and 28, arose from incomplete stripping of earlier probes. With probes 8 and 9, species I (full-length *lysT* operon) was detected in the *rnpA49 rph-1* strain, while species I and II were present in the *rne-1 rnpA49 rph-1* strain (lanes 17–20; data not shown). These results suggested that species II was generated by RNase E cleavage between the *lysZ* and *lysQ* tRNAs, since it hybridized with probes 8 and 9, but not 10 or 11 (lanes 20, 28).

Similarly, species III arose from a cleavage between *lysY* and *lysZ* tRNAs based on its hybridization to probes 5 and 6, but not the probes 8 and 9 (lanes 13–20, data not shown). Species IV was most likely a *lysT valT lysW valZ* processing intermediate because of its molecular weight, but we could not unequivocally make this assignment.

Based on the data shown in Figure 1, the hybridization of probe f to species V in both the *rnpA49 rph-1* and *rne-1 rnpA49 rph-1* mutants (Figure 2B, lanes 2 and 4), represented the detection of the full-length *valU* polycistronic transcript. The failure of probe 1 (Figure 2A) to hybridize to species V (Figure 2B, lanes 6 and 8) confirmed this identification. However, probe 1 hybridized to the two most prominent species of ~430 and ~140 nt (VIA and XII), respectively, in the *rnpA49 rph-1* double mutant (Figure 2B, lane 6). Since species VIA also hybridized to probes 2 and 4 (Figure 2A, B, lanes 10, 22), but not to probe 5 (Figure 2B, lane 14), this species was identified as *lysT valT lysW* processing intermediate that retained its 5′ leader region.

Species XII was identified as a *lysT* intermediate with the 5′ leader region, since it hybridized to probes f and 1 (Figure 2A and B, lanes 2, 6). The intensities of VIA and XII decreased significantly in the *rne-1 rnpA49 rph-1* triple mutant (Figure 2B, lane 8 versus lane 6) along with con-

comitant increases in the intensities of species I-IV, suggesting these processing intermediates arose from RNase E cleavages within the larger *lysT* polycistronic transcript. It should be noted that species VIA (*lysT valT lysW*) is similar in size to species VI (Figure 1B, *valU valX valY lysV*).

Species VIIA was observed with probes that were complementary to the spacer region between *lysT* and *valT* (probes 2, 3) (Figure 2B, lanes 10, 12; data not shown), but was not detected with a probe complementary to the intergenic region between *valT* and *lysW* (probe 4) (Figure 2B, lanes 22, 24). Thus, species VIIA was a *lysT valT* processing intermediate that retained its 5′ terminal sequence. It was designated as VIIA to distinguish it from species VII that was observed in Figure 1B, but was a *valU valX valY* processing intermediate that was almost identical in size. Species XIII was only observed with probe f (Figure 2B, lane 2) and probe 9 (data not shown), suggesting it was a *lysZ* intermediate that retained some 3′ sequences.

Species X hybridized to probe 4 (Figure 2A and B, lanes 2, 22) as well as probe 7 (data not shown). However, it failed to hybridize with probes 2, 5 and 8 (Figure 2B, lanes 10, 14 and 18). Thus, this species seemed to be a mixture of *valT lysW* and *valZ lysY* intermediates. The absence of species X in the *rne-1 rnpA49 rph-1* triple mutant indicated that these intermediates were generated by RNase E cleavages upstream of *valT, valZ* and *lysZ* in the absence of RNase P.

Identification of cleavage sites using RNA circularization

Although the data in Figures 1 and 2 clearly identified the composition of the various tRNA processing intermediates from the *valU* and *lysT* operons, the Northern analyses did not provide insights into the precise cleavage sites. Since primer extension analysis was not technically feasible for these two polycistronic transcripts, we employed cloning and sequencing of cDNAs derived from reverse transcription of self-ligated tRNAs (29) to identify the 5′ and 3′ termini of various species. This method has been successfully employed previously to simultaneously obtain the 5′ and 3′ termini of specific individual tRNA species (15,28).

Accordingly, clones were obtained from *rph-1, rnpA49 rph-1* and *rne-1 rnpA49* strains and sequenced (see Materials and Methods). The data presented in Figure 3, represent the analysis of over 150 independent isolates obtained from the three genetic backgrounds. Although it was not possible to obtain sequence information for every cleavage site, we were able to identify RNase P cleavages at the mature 5′ termini of the *valU*, *valX*, *valY, lysV* and *lysW* transcripts (Figure 3, P1–5), since there are no known 5′ → 3′ exonucleases in *E. coli*. Furthermore, it appeared that RNase P and perhaps RNase E cleaved two nucleotides downstream of the CCA of *lysV* to remove the Rho-independent transcription terminator from the polycistronic *valU* primary transcript (T5, Figure 3). It should also be noted that the transcription start-site (TSS) of the *valU* operon is 9 nt upstream of the mature 5′ terminus of *valU* (Figure 3), not 7 nt as indicated at the EcoCyc Website. The identification of various 5′ and 3′ ends (Figure 3) was consistent with several processing intermediates (M, VI, VII, VIII, XI and X) that had been characterized by Northern analysis (Figures 1 and 2).

### RNase P is the only enzyme that generates valine pre-tRNAs

In order to further confirm that RNase P was both essential and sufficient for the generation of the valine pre-tRNAs, we carried out half-life measurements on the three large *valU* operon species (Figure 1B, V, VI and VII). We predicted that if other endoribonucleases were involved in processing this polycistronic transcript, even inefficiently, we would see the decay of one or more of these species in an *rnpA49 rph-1* double mutant. In the *rph-1* control, both species V (the full-length transcript) and VII (*valU valX valY*) had identical half-lives of ~1 min (Figure 4, Table 2), while the half-life of species VI was estimated at <0.5 min (Figure 4, Table 2). In the *rne-1 rph-1* mutant, all three species had half-lives of <0.5 min (Figure 4, Table 2), explaining the higher RQ and PF values of steady-state *valU* tRNAs compared to the *rph-1* strain (Figure 1B, lanes 1, 2). Although the exact reason for faster processing of the *valU* transcript in the *rne-1 rph-1* double mutant is not clear, it might simply be due to better access of RNase P to its processing sites in the absence of RNase E.

In contrast, in the absence of RNase P, the half-life of species V increased over 7-fold, while that of species VI and VII increased over 30-fold (Figure 4, Table 2). In the absence of both RNase E and RNase P, all three species had half-lives of >30 min. These data provided further support that normally RNase P catalyzes the initial removal of the Rho-independent transcription terminator from the *valU* transcript. However, in the absence of RNase P, RNase E can substitute inefficiently to carry out this reaction.

Since the *lysT* polycistronic transcript is over 1100 nt in length, we carried out half-life experiments for this operon using 1.2% agarose gels. Unlike what was observed with the full-length *valU* transcript, we could not detect the full-length *lysT* transcript in either the *rph-1* or *rne-1 rph-1* strains even at time zero, indicating a half-life of <0.5 min in these genetic backgrounds (data not shown). In contrast, the half-life of species I was >30 min in an *rne-1 rnpA49 rph-1* triple mutant (Table 2).

Although these data strongly suggested that RNase P was primarily responsible for the initial processing of all five valine type 1 tRNAs, we wanted to directly rule out the possibility that other known ribonuclease(s) besides RNase E might be involved in their processing. Accordingly, we tested a variety of multiple mutants that were deficient in RNase III (*rnpA49 rnc-14 rph-1*), RNase G (*rne-1 rnpA49 Δrng rph-1*), RNase LS (*rne-1 rnpA49 rnlA2 rph-1*), YbeY (*rnpA49 ΔybeY rph-1*) and RNase Z (*rne-1 rnpA49 Δrnz rph-1*) as well as either RNase P or RNase E. None of the additional endonucleases tested affected the processing of the *valU* operon (data not shown). We also eliminated the possibility of residual RNase E activity in strains carrying the *rne-1* allele (15) by examining *valU* operon processing in an RNase E deletion strain [*rnpA49 Δrne-1018/ rng-219 rph-1*, data not shown, see (32)].

Since species VII (*valU valX valY,* Figure 1) was present in both the *rnpA49 rph-1* and *rne-1rnpA49 rph-1* strains, we also tested the possibility that the *lysV* tRNA was removed by exonucleolytic processing from the 3′ terminus. However, the processing of the *valU* primary transcript in multiple mutant strains deficient in PNPase (*pnp*) and RNase II
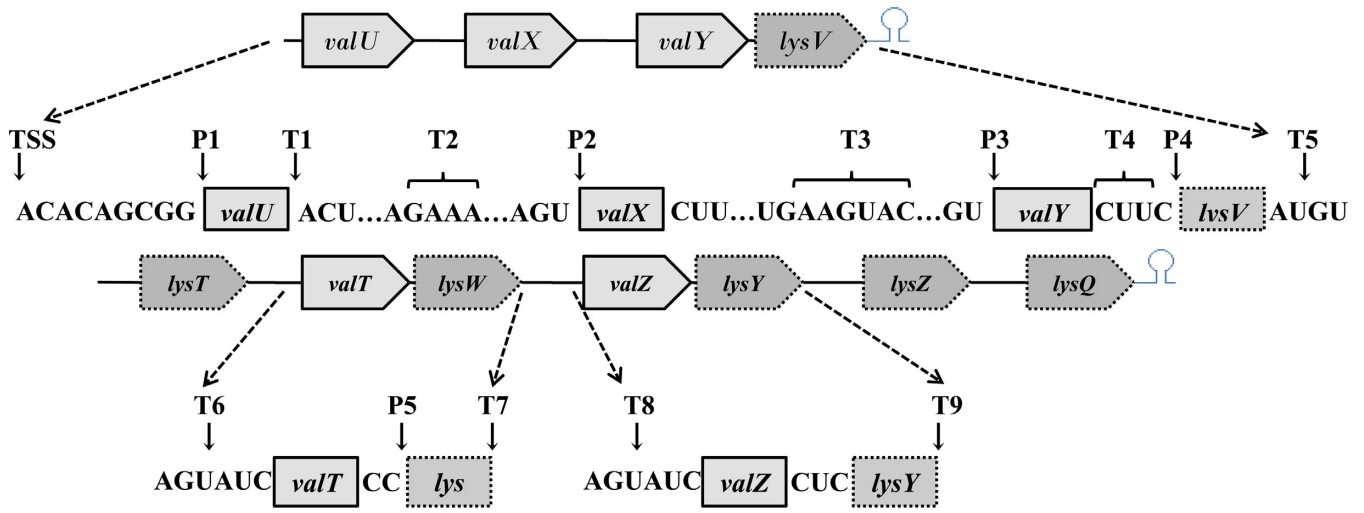
Cloned Fragment	Northern Intermediate	Source of Origin
P1-T1	M	*valU valX valY lysV*
TSS – T5	VI	*valU valX valY lysV*
TSS – T4	VII	*valU valX valY lysV*
TSS – T3	VIII	*valU valX valY lysV*
TSS – T1	XI	*valU valX valY lysV*
T3-T5	X	*valU valX valY lysV*
T6 – T7	X	*lysT valT lysW valZ lysY lysZ lysQ*
T8 – T9	X	*lysT valT lysW valZ lysY lysZ lysQ*

Figure 3. Identification of cleavage sites within the *valU* and *lysT* operons by cloning and sequencing of processing intermediates. cDNAs of self-ligated RNA molecules were amplified, cloned and sequenced to identify the 5′ and 3′ ends as described in 'Materials and Methods'. Each arrow represents either a 5′ or 3′ end based on the DNA sequence. Multiple ends were obtained at the T2, T3 and T4 locations. The transcription, start-site (TSS), RNase P cleavage sites (P1–5), 3′ cleavage sites [either at the mature 3′ end or in the intergenic region for respective upstream tRNAs (T1–5, 7 and 9)] and 5′ cleavage sites (in the intergenic regions) for respective downstream tRNAS (T6, 8) are indicated. The 3′ and 5′ ends of some of the major processing intermediates observed in the Northern analyses (Figures 1 and 2) are shown below the diagram.
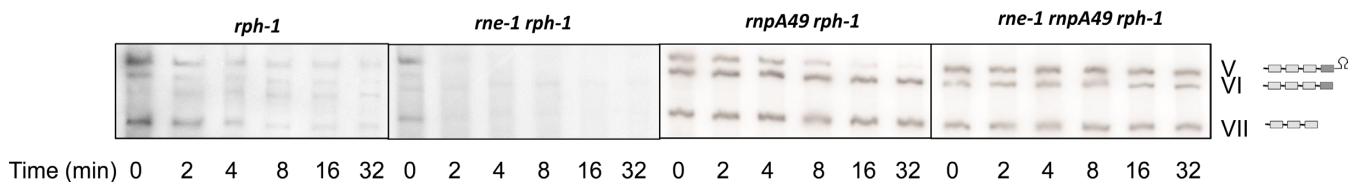

Figure 4. Northern analysis of the decay of *valU* operon. The genotypes of the strains are indicated on the top and time-points are shown at the bottom of the autoradiograms. The blots were probed with probe b (Figure 1A). The numerical designations of the different species with their graphical structures are shown to the right and are identical to those shown in Figure 1.

Table 2. Half-lives of *valU* and *lysT* operon transcripts in various strains

(A) *valU*

Species	Half-life (min)			
	rph-1	*rnpA49 rph-1*	*rne-1 rph-1*	*rne-1 rnpA49 rph-1*
V	1.0 ± 0.4	7.7 ± 1.4	<0.5	>30
VI	<0.5	>30	<0.5	>30
VII	1.1 ± 0.1	>30	<0.5	>30

(B) *lysT*

Species	Half-life (min)			
	rph-1	*rne-1 rnpA49 rph-1*	*rnpA49 rne∆1019 rng-219 rph-1*	*rne-1 rnpA49 ∆rnz ∆rng rnlA2 rph-1*
I	<0.5	>30	>30	>30

Species designations are as indicated in Figures 1 and 2. Half-lives were determined as described in the ′Materials and Methods'. Data reflect the averages of at least three independent determinations.

(*rnb*) (*rne-1 pnp-7 rnb-500 rph-1*; *rnpA49 pnp-7 rnb-500 rph-1*; and *rne-1 rnpA49 rnb-500 pnp-7,rph-1*), was unchanged compared to a *rnpA49 rph-1* strain (data not shown).

Ectopic expression of mature valine tRNAs does not suppress the inviability associated with an *rnpA49* mutant

Because the loss of RNase P results in tRNAs with immature 5′ ends, it has been assumed that such pre-tRNAs cannot be aminoacylated leading to an inhibition of protein synthesis and a subsequent loss of cell viability. However, recent studies suggest that tRNAs with immature 5′ but mature 3′ ends can be functional both *in vivo* and *in vitro* (15). Alternatively, the loss of RNase P activity could be lethal if all of a particular species of tRNA(s) remained as unprocessed primary transcripts. From the analysis of the processing of the *valU* and *lysT* operons (Figures 1 and 2), it was evident that the amount of mature tRNA[Val(UAC)] was reduced >4-fold in an *rnpA49 rph-1* strain. Since the processing of tRNA[Val(GAC)] is also completely dependent on RNase P (17), we hypothesized that the loss of cell viability in the absence of RNase P might arise from the significantly reduced levels of functional valine tRNAs [Figure 1B, lane 3; (17)].

In order to test this hypothesis directly, we generated a set of compatible plasmids from which the two valine isotypes, tRNA[val(GAC)] (*valW*) and tRNA[val(UAC)] (*valU*) were ectopically expressed in a way that did not require RNase P processing at either the 5′ or 3′ terminus. In both cases, the *valW* and *valU* genes were constructed such that transcription termination was controlled by the *leuU* Rho-independent transcription terminator, which is known to be removed efficiently by RNase E (15). Furthermore, to eliminate the need for RNase P processing of the tRNAs synthesized from the plasmids, they were designed such that transcription initiated at the mature 5′ terminus of each tRNA.

To ensure that the tRNA species being expressed from the two plasmids were mature and functional, we measured the *in vivo* aminoacylation levels of the two valine tRNA isotypes. Surprisingly, the percentage of aminoacylation of both the valine tRNA isotypes was less than 40% in an *rph-1* strain (Table 3). This result was unexpected since other tRNAs have charging efficiencies ranging between 60 and

90% (33,34) in the same genetic background. Surprisingly, the level of aminoacylation improved only marginally in the *rph⁺* strain in spite of the significant improvement in 3′ end maturation (Figure 1C). As expected, the extent of aminoacylation of both valine tRNAs decreased between 1.9 and 2.3-fold (Table 3) in the absence of RNase P, but the aminoacylation levels of both tRNAs returned to the level observed in the *rph-1* control upon ectopic expression of both tRNAs from plasmids in an *rnpA49 rph-1* strain (Table 3).

Subsequently, we measured the growth and cell viability of an *rnpA49 rph-1* strain in which both valine tRNAs were ectopically expressed. As a positive control we also overexpressed the M1 RNA component of RNase P, since increased levels of the M1 RNA have been shown to partially complement the *rnpA49* allele at 42°C (35,36). As shown in Figure 5, the simultaneous expression of tRNA[val(GAC)] and tRNA[val(UAC)] did not suppress the temperature sensitivity of the *rnpA49* strain. In contrast, overproduction of the *rnpB* gene did lead to a small improvement in the growth of the *rnpA49 rph-1* strain at 42°C. In addition, there was no change in cell viability in the strain ectopically expressing both mature valine tRNAs (data not shown). It should be noted that identical results were obtained in an *rnpA49 rph⁺* strain (data not shown).

Ectopic expression of the mature 4.5S RNA or tRNA[Arg(CCG)] does not suppress the inviability associated with the *rnpA49* allele

It has previously been suggested that overexpression of tRNA[Arg(CCG)] can complement an *rnpA49* mutation (35). However, as shown in Figure 5, ectopic expression of this tRNA had no effect on the growth of an *rnpA49 rph-1* mutant at the elevated temperature. It is known that RNase P is required to generate the mature 5′ end of the essential 4.5S RNA (8). In fact, it has been suggested that this processing reaction could be the essential function of RNase P in *E. coli* (37). Accordingly, we expressed a 4.5S RNA species from a plasmid that did not require RNase P processing at it 5' terminus. Increased levels of this species also did not suppress the conditional lethality of the *rnpA49* allele (data not shown).

Table 3. Aminoacylation levels of mature valine tRNAs

tRNA isotype/genes	Percentage of aminoacylated tRNA			
	rph-1	*rnpA49 rph-1*	*rnpA49 rph-1/valU$^+$ valW$^+$*	*rph$^+$*
Val1/*valU, X, Y, T, Z*	39 ± 2	17 ± 6	37 ± 3	41 ± 5
Val2/*valV, W*	38 ± 4	20 ± 3	37 ± 3	47 ± 5

The percentage of each aminoacylated tRNA was determined by the method of Varshney (27) as previously described (33). *valU$^+$* and *valW$^+$* represent tRNA species transcribed from plasmids pAAK11 and pAAK13, respectively as 5′-mature molecules with a *leuU* transcription terminator known to be removed efficiently by RNase E (15) (See Materials and Methods). Data shown are the average of at least two independent determinations.
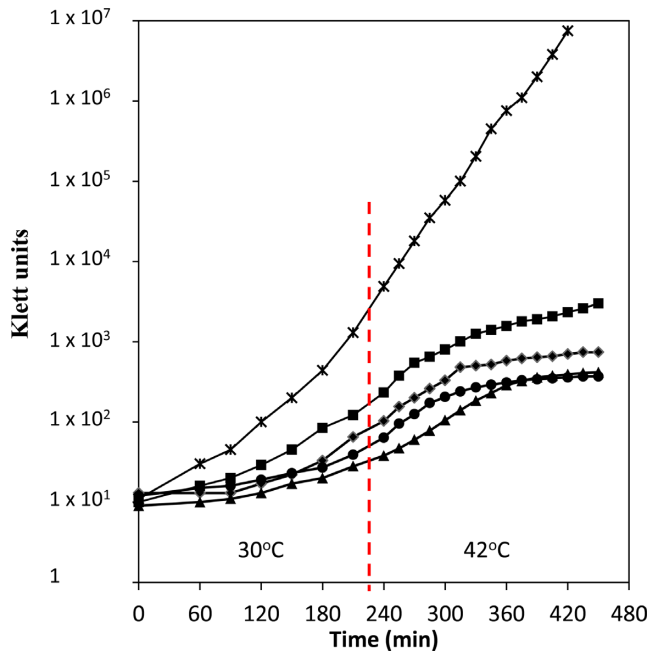

Figure 5. Growth curve of various strains. All strains were initially grown at 30°C until 50 Klett units above background when IPTG was added to a final concentration of 350 μM. The cultures were diluted with pre-warmed Luria broth (LB)/thymine or LB/thymine/IPTG to maintain them in exponential growth (Klett 50–70). For this experiment, all the cultures were shifted to 42°C when the slowest growing culture reached Klett 50 above background (vertical dashed line), since it has been previously shown that overproduction of *rnpB* does not complement at 44°C (36). The optical densities (OD) were measured with a Klett-Summerson Colorimeter (No. 42 Green filter). x: MG1693 (*rph-1*); ◆: SK2525 (*rnpA49 rph-1*); ▲: SK10537 (*rnpA49 rph-1 argX$^+$*); ●: SK10541 (*rnpA49 rph-1 valU$^+$ valW$^+$*); ■: SK10539 (*rnpA49 rph-1 rnpB$^+$*).

DISCUSSION

The data presented here demonstrate that all five of the valine isotype 1 pre-tRNAs derived from the *valU* and *lysT* operons are initially generated by RNase P cleavages (Figures 1 and 2). When coupled with our previous work showing that the two valine isotype 2 tRNAs (*valV* and *valW*) also exclusively use RNase P for their initial processing (17), it is clear that all seven valine tRNA species in *E. coli* require RNase P for separation from their primary polycistronic transcripts. The more than 4-fold decrease in the level of mature valine tRNA after shift to the non-permissive temperature was consistent with the absolute requirement for initial RNase P cleavages [Figure 1, (17)].

What is most striking about the results presented here relates to how RNase P processes both the *valU* and *lysT* polycistronic transcripts. There are three possible mechanisms by which RNase P could process the primary transcripts: (i) initiate cleavage at the 5′ terminus of the first tRNA in the operon and proceed in the 5′ → 3′ direction to the end of the transcript; (ii) initiate processing by first removing the Rho-independent transcription terminator and proceeding in the 3′ → 5′ direction to the 5′ proximal end of the transcript; or (iii) cleave the transcripts randomly with some sites being preferred over others.

These three possibilities can be distinguished by examining the processing intermediates obtained in the various *rnpA49* mutants (Figures 1 and 2). For example, in the case of the *valU* operon, all of the major processing intermediates observed after inactivation of RNase P retained their immature 5′ termini (Figure 1B, lanes 3, 7). These data clearly rule out RNase P initiating cleavage at the 5′ proximal terminus and proceeding in the 5′ → 3′ direction. In addition, both Northern analysis and cDNA sequencing of processing intermediates suggested that each of the intermediates detected in the *rnpA49 rph-1* mutant was shortened by one tRNA (Figure 1B, species VI, VII, VIII and XI: Figure 3). It would thus appear that the separation of the *valU* polycistronic transcript is not random but rather proceeds in the 3′ → 5′ direction, as outlined in Figure 6, with the first cleavage reaction being the removal of the Rho-independent transcription terminator. This is in contrast to the processing of the *valV valW* dicistronic transcript, where it was suggested that RNase P cleavage at the 5′ terminus of *valW* tRNA might occur cotranscriptionally, since computational models of the dicistronic transcript indicated that this RNase P site might be occluded (17).

Furthermore, the data shown in Figures 1 and 4 demonstrate that the only role RNase E plays in the processing of the *valU* operon is to inefficiently remove the Rho-independent transcription terminator in the absence of RNase P, since the processing pattern of the full-length transcript remained unchanged in the *rne-1 rph-1* mutant compared to the *rph-1* single mutant except for the slightly reduced signal intensity of species V (Figure 1B, lanes 1, 2). The half-life data (Figure 4) and our analysis of other multiple mutants lacking RNase III, RNase G, YbeY, RNase Z and RNase LS (data not shown) also confirmed that RNase P was the only endonuclease that processed the full-length *valU* transcript and thus was primarily responsible for the removal of the Rho-independent transcription terminator. These results were also very different from what was observed with the *metT* operon in which inactivation of RNase
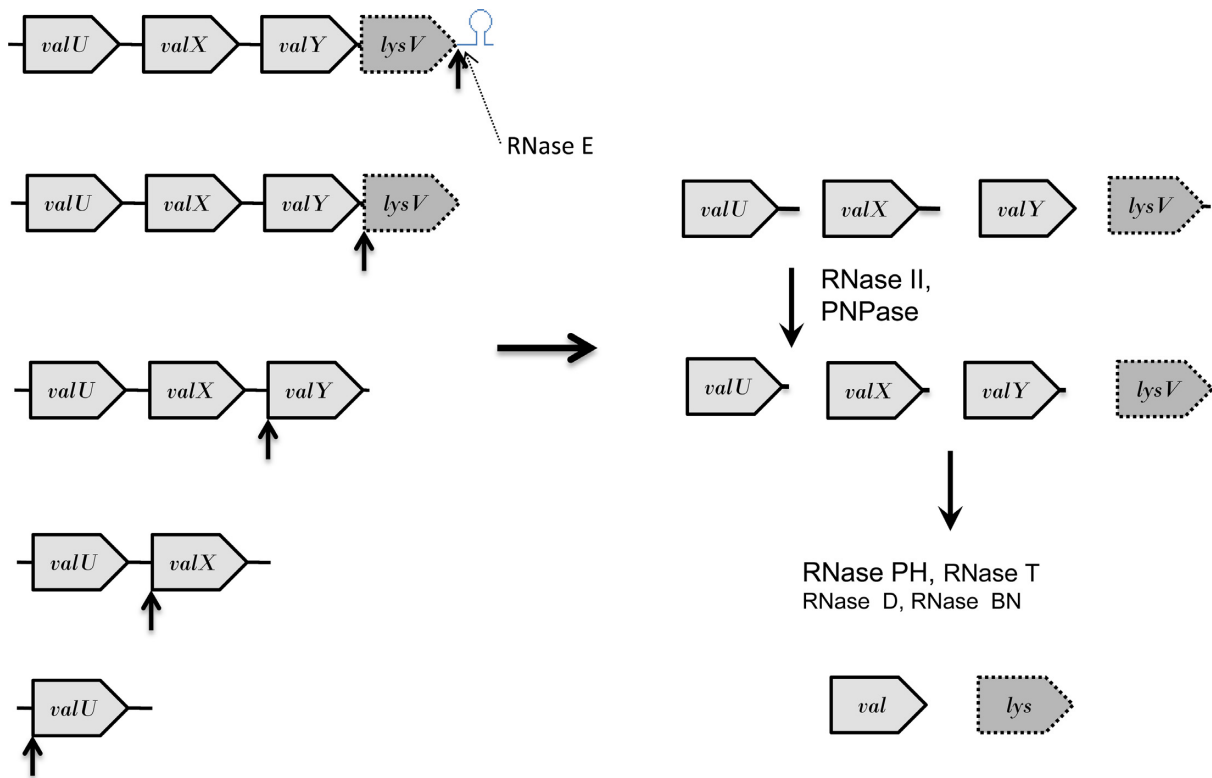
Figure 6. Processing pathway for the *valU* polycistronic transcript. Similar to what has been observed with the *valV valW* and *secG leuU* primary transcripts (15,17), RNase P (upward black arrows) is the primary processing enzyme for the *valU* transcript. Initially, RNase P efficiently removes the Rho-independent transcription terminator (upward black arrow). Subsequent sequential cleavages occur in the 3′ → 5′ direction at the mature 5′ termini of *lysV*, *valY*, *valX* and *valU* (upward black arrows). The *valU* and *valX* pre-tRNAs will have long 3′ termini of 44 and 47 nt, respectively (Figure 1A) that will be initially processed by a combination of RNase II and PNPase (17,48). Subsequently, the final processing of the valine pre-tRNAs will be carried out primarily by RNase PH because of the presence of C residues downstream of the CCA determinant (42). The final processing of the *lysV* pre-tRNA employs RNase T. In the absence of RNase P, RNase E can inefficiently remove (dashed arrow) the Rho-independent transcription terminator (Figure 1B). Transcripts are not drawn to scale.

E by itself led to a significant change in the observed processing intermediates (15).

The processing of the *lysT* operon is somewhat more complex. On the one hand, RNase E does not play a significant role in the separation of any of the seven tRNAs in the presence of RNase P as judged by the lack of any new decay intermediates in the *rne-1 rph-1* strain (Figure 2B, lane 3). Furthermore, as seen with the *valU* operon, the vast majority of the processing intermediates in both the *rnpA49 rph-1* and *rne-1 rnpA49 rph-1* strains retained their 5′ termini, again suggesting that RNase P initiates the processing of the large 1100 nt transcript at the 3′ and proceeds in the 3′→ 5′ direction. The increase in the amounts of species I–IV in the *rne-1 rnpA49 rph-1* triple mutant can be ascribed to the ability of RNase E to cleave within the large spacer regions between *lysT* and *valT* (135 nt), *lysW* and *valZ* (150 nt), *lysY* and *lysZ* (147 nt), and *lysZ* and *lysQ* (133 nt) (Figure 2A) in the absence of RNase P due to stabilization of the primary transcript. The identification of *valT lysW* and *valZ lysY* intermediates with 5′ unprocessed ends (Figure 3) is consistent with this analysis. These cleavages do not occur in the presence of RNase P (Figure 2B, lane 3), since each of the tRNAs is processed at the 5′ mature terminus (Figure 7). Thus, we propose a processing pathway for the *lysT*

operon (Figure 7), which is similar to that described for the *valU* operon (Figure 6).

The data presented above suggest that transcription must be complete before any processing occurs, indicating that nascent transcripts are initially protected from degradation. Although the basis of this protection is not clear, it is possible that either the secondary structure of the transcript itself or RNA chaperones like Hfq (38) prevent processing until the entire transcript is completed. Taken together, our data indicate that RNase P can efficiently process large transcripts starting from their 3′ termini *in vivo*. In fact, based on the half-life data (Table 2), the enzyme works more efficiently on the 1100 nt *lysT* transcript than the 440 nt *valU* transcript. These results are consistent with the fact that RNase P cleaves the 5′ end of a tRNA poorly in the presence of a long 3′ trailer (39).

It should also be noted that Hansen *et al.* (40) showed that RNase P could cleave single-stranded oligonucleotides *in vitro* particularly between U and G. Moreover, Mohanty and Kushner (7) demonstrated that the Rho-independent transcription terminator associated with the *leuX* transcript was removed *in vivo* by an RNase P cleavage reaction between a U and G residue seven nucleotides downstream of the CCA determinant. It is thus not surprising that the Rho-independent transcription terminator associated with
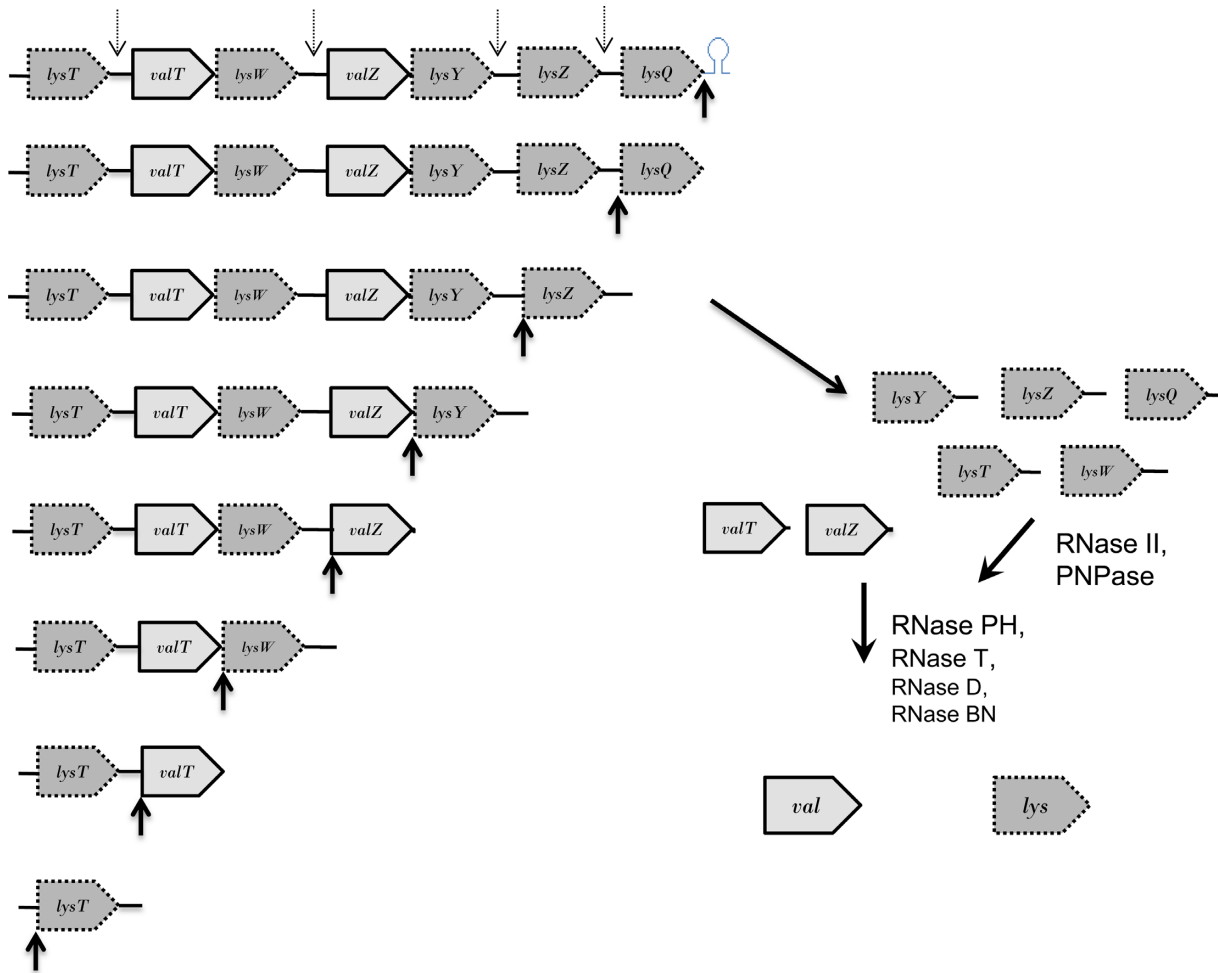
Figure 7. Processing pathway for the *lysT* polycistronic operon. Similar to what was described in Figure 6, after RNase P removes the Rho-independent transcription terminator (upward black arrow), subsequent sequential cleavages will occur in the 3′ → 5′ direction at the mature 5′ termini of *lysQ*, *lysZ*, *lysZ*, *lysW*, *valT* and *lysT* (upward black arrows) to generate pre-tRNAs containing between 2 and150 nt extra nucleotides at their 3′ ends (Figure 2A). The long 3′ ends of the five *lys* pre-tRNAs will be initially processed by a combination of RNase II and PNPase (17,48). Final maturation of the *lys* tRNAs primarily is carried out by RNase T, while the final processing of the two valine species is done by RNase PH. In the absence of RNase P, RNase E (dashed downward arrows) can cleave within the long spacer regions between *lysT* and *valT*, *lysW* and *valZ*, *lysY* and *lysZ*, *and lysZ* and *lysQ*. However, RNase E does not separate *valT* and *lysW* or *valZ* and *lysY*. Transcripts are not drawn to scale.

the *valU* operon was also removed endonucleolytically by an RNase P cleavage between a U and G residue three nucleotides downstream of the CCA (Figure 3). Furthermore, since the terminators of both the *valU* and *lysT* operons have identical sequences, it is presumed that the Rho-independent transcription terminator associated with the *lysT* operon is removed in a similar fashion.

However, the model shown in Figure 6 does not completely explain the origin of species VII (*valU valX valY*), which was present in all the genetic backgrounds (Figure 1B, lanes 1–4). Since there is only a four nucleotide spacer between *valY* and *lysV* (CUUC), this sequence should not be cleaved by RNase E (30,31). Yet there is an almost 2-fold decrease in the amount of this species in the *rne-1 rnpA49 rph-1* triple mutant and the *rne-1 rnpA49 Δrnz Δrng rnlA2 rph-1* hextuple mutant (data not shown) compared to the *rnpA49 rph-1* double mutant (Figure 1B, lanes 3, 4). Thus, it is possible that RNase E is cleaving poorly in between *valY* and *lysV* (ACCACUUC). In addition, we could

not demonstrate any exonucleolytic removal of *lysV* tRNA from the full-length transcript, similar to the removal of the *leuX* Rho-independent transcription terminator by PNPase (7). Thus, another possibility is that this species arises from premature transcription termination at a site immediately downstream of *valY*. Alternatively, it is possible that there is another endonuclease, as yet unidentified.

Based on the absolute dependence on RNase P for the initial separation of all seven valine tRNAs [Figures 1 and 2, (17)], we hypothesized that ectopic expression of both valine isotypes in a fashion that did not require RNase P to generate mature species might suppress the lethality associated with the *rnpA49* mutation. To our surprise, even though ectopic expression of the two valine tRNAs led to a significant increase in the amount of aminoacylated valine tRNAs (Table 3), no suppression of the growth defect was observed (Figure 5). In fact, when both valine tRNAs were simultaneously expressed, the strain grew more slowly than the *rnpA49* mutant on its own (Figure 5). The only improve-

ment in growth in the *rnpA49* mutant after shift to 42°C occurred in the presence of increased expression of the M1 RNA, in agreement with previously reported results (36). Furthermore, we were not able to reproduce the work of Kim *et al.* (35), who suggested that overproduction of an arginine tRNA could suppress the *rnpA49* allele. In addition, we also ruled out the possibility that the processing of the 5′ end of the 4.5S RNA was the essential function of RNase P (data not shown).

Since it has been reported that the dephosphorylation of the 5′ triphosphate by the RppH enzyme from *Bacillus subtilis* requires a single-stranded region of at least two nucleotides (41), it is possible that the ectopically expressed RNAs retained their 5′ triphosphates. Although the data in Table 3 demonstrate that the potential presence of a triphosphate did not interfere with aminoacylation, we cannot rule out the possibility that the triphosphate moiety at the 5′ terminus of the charged tRNA interfered with its binding to the ribosome.

Finally, it should be noted that the final maturation of the 3′ termini of the valine type 1 tRNAs required RNase PH (Figure 1C), while the type II valine tRNAs (17) and the lysine tRNAs (Figure 2) did not. These observations are in agreement with the results of Zuo and Deutscher (42) who showed that C nucleotides immediately downstream of the CCA determinant will inhibit RNase T activity. In the case of the type I valine tRNAs, four of the five species have at least one C immediately downstream of the CCA (CCAACUAC, CCACUUUC, CCACUUC, CCACC, CCACUC). In contrast, this is not the case with the *valV* and *valW* transcripts (CCAUCCU, CCAGAUU) or all six *lys* transcripts (data not shown). It is also worth noting that even though the presence of wild-type RNase PH activity led to a single mature *val* tRNA species (Figure 1C), the fraction of aminoacylated type 1 tRNA did not significantly increase (Table 3, data not shown). Thus, the relatively low levels of valine aminoacylation are not related to 3′ end processing but rather to inefficient charging.

SUPPLEMENTARY DATA

Supplementary Data are available at NAR Online. Supplementary Table S1

ACKNOWLEDGMENTS

FUNDING

REFERENCES

1. Blattner,F.R., Plunkett,G. III, Bloch,C.A., Perna,N.T., Burland,V., Riley,M., Collado-Vides,J., Glasner,J.D., Rode,C.K.,, Mayhew,G.F. *et al.* (1997) The complete sequence of *Escherichia coli* K-12. *Science*, **277**, 1453–1474.

2. Berlyn,M.K.B. (1998) Linkage map of *Escherichia coli* K-12, edition 10: the traditional map. *Microbiol. Mol. Biol. Rev.*, **62**, 814–984.

3. Li,Z. and Deutscher,M.P. (2002) RNase E plays an essential role in the maturation of *Escherichia coli* tRNA precursors. *RNA*, **8**, 97–109.

4. Ow,M.C. and Kushner,S.R. (2002) Initiation of tRNA maturation by RNase E is essential for cell viability in *E. coli. Genes Dev.*, **16**, 1102–1115.

5. Deutscher,M.P. (2006) Degradation of RNA in bacteria: comparison of mRNA and stable RNA. *Nucleic Acids Res.*, **34**, 659–666.

6. Li,Z. and Deutscher,M.P. (1996) Maturation pathways for *E. coli* tRNA precursors: a random multienzyme process *in vivo. Cell*, **86**, 503–512.

7. Mohanty,B.K. and Kushner,S.R. (2010) Processing of the *Escherichia coli leuX* tRNA transcript, encoding tRNA^leu5^, requires either the 3′−5′ exoribonuclease polynucleotide phosphorylase or RNase P to remove the Rho-independent transcription terminator. *Nucleic Acids Res.*, **38**, 597–607.

8. Sakano,H., Yamada,S., Ikemura,T., Shimura,Y. and Ozeki,H. (1974) Temperature sensitive mutants of *Escherichia coli* for tRNA synthesis. *Nucleic Acids Res.*, **1**, 355–371.

9. Stark,B.C., Kole,R., Bowman,E.J. and Altman,S. (1978) Ribonuclease P: an enzyme with an essential RNA component. *Proc. Natl Acad. Sci. U.S.A.*, **75**, 3717–3721.

10. Brown,S. and Fournier,M.J. (1984) The 4.5 S RNA gene of Escherichia coli is essential for cell growth. *J. Mol. Biol.*, **178**, 533–550.

11. Bothwell,A.L., Stark,B.C. and Altman,S. (1976) Ribonuclease P substrate specificity: cleavage of a bacteriophage phi80-induced RNA. *Proc. Natl Acad. Sci. U.S.A.*, **73**, 1912–1916.

12. Alifano,P., Rivellini,F., Piscitelli,C., Arraiano,C.M., Bruni,C.B. and Carlomagno,M.S. (1994) Ribonuclease E provides substrates for ribonuclease P-dependent processing of a polycistronic mRNA. *Genes Dev.*, **8**, 3021–3031.

13. Li,Y., Cole,K. and Altman,S. (2003) The effect of a single, temperature-sensitive mutation on global gene expression in *Escherichia coli. RNA*, **9**, 518–532.

14. Phizicky,E.M. and Hopper,A.K. (2010) tRNA biology charges to the front. *Genes Dev.*, **24**, 1832–1860.

15. Mohanty,B.K. and Kushner,S.R. (2008) Rho-independent transcription terminators inhibit RNase P processing of the *secG leuU* and *metT* tRNA polycistronic transcripts in *Escherichia coli. Nucleic Acids Res.*, **36**, 364–375.

16. Perret,V., Florentz,C. and Giege,R. (1990) Efficient aminoacylation of a yeast transfer RNA^Asp^ transcript with a 5′ extension. *FEBS Lett.*, **270**, 4–8.

17. Mohanty,B.K. and Kushner,S.R. (2007) Ribonuclease P processes polycistronic tRNA transcripts in *Escherichia coli* independent of ribonuclease E. *Nucleic Acids Res.*, **35**, 7614–7625.

18. Keseler,I.M., Collado-Vides,J., Santos-Zavaleta,A., Peralta-Gil,M., Gama-Castro,S., Muniz-Rascado,L., Bonavides-Martinez,C., Paley,S., Krummenacker,M., Altman,T. *et al.* (2011) EcoCyc: a comprehensive database of *Escherichia coli* biology. *Nucleic Acids Res.*, **39**, D583–D590.

19. Schedl,P. and Primakoff,P. (1973) Mutants of *Escherichia coli* thermosensitive for the synthesis of transfer tRNA. *Proc. Natl Acad. Sci. U.S.A.*, **70**, 2091–2095.

20. Ono,M. and Kuwano,M. (1979) A conditional lethal mutation in an *Escherichia coli* strain with a longer chemical lifetime of mRNA. *J. Mol. Biol.*, **129**, 343–357.

21. Mohanty,B.K. and Kushner,S.R. (1999) Analysis of the function of *Escherichia coli* poly(A) polymerase I in RNA metabolism. *Mol. Microbiol.*, **34**, 1094–1108.

22. Grana,D., Gardella,T. and Susskind,M.M. (1988) The effects of mutations in the *ant* promoter of phage P22 depend on context. *Genetics*, **120**, 319–327.

23. Kushner,S.R. (1978) In: Boyer,HW and Nicosia,S (eds). *Genetic Engineering*. Elsevier/North-Holland Biomedical Press, Amsterdam, pp. 17–23.

24. Bertani,G. (1951) Studies on lysogenesis. I. The mode of phage liberation by lysogenic *Escherichia coli. J. Bacteriol.*, **62**, 293–300.

25. Mohanty,B.K., Giladi,H., Maples,V.F. and Kushner,S.R. (2008) Analysis of RNA decay, processing, and polyadenylation in *Escherichia coli* and other prokaryotes. *Methods Enzymol.*, **447**, 3–29.

26. Stead,M.B., Agarwal,A., Bowden,K.D., Nasir,R., Meagher,R.B., Mohanty,B.K. and Kushner,S.R. (2012) RNAsnap^TM : a rapid, quantitative, and inexpensive, method for isolating total RNA from bacteria. *Nucleic Acids Res.*, **40**, e156.

27. Varshney,U., Lee,C.P. and RajBhandary,U.L. (1991) Direct analysis of aminoacylation levels of tRNAs *in vivo*. Application to studying recognition of *Escherichia coli* initiator tRNA mutants by glutaminyl-tRNA synthetase. *J. Biol. Chem.*, **266**, 24712–24718.

28. Mohanty,B.K., Maples,V.F. and Kushner,S.R. (2012) Polyadenylation helps regulate functional tRNA levels in *Escherichia coli*. *Nucleic Acids Res.*, **40**, 4589–4603.

29. Mohanty,B.K. and Kushner,S.R. (2014) In vivo analysis of polyadenylation in prokaryotes. *Methods Mol. Biol.*, **1125**, 229–249.

30. McDowall,K.J., Lin-Chao,S. and Cohen,S.N. (1994) A + U content rather than a particular nucleotide order determines the specificity of RNase E cleavage. *J. Biol. Chem.*, **269**, 10790–10796.

31. Kaberdin,V.R. (2003) Probing the substrate specificity of *Escherichia coli* RNase E using a novel oligonucleotide-based assay. *Nucleic Acids Res.*, **31**, 4710–4716.

32. Chung,D.-H., Min,Z., Wang,B.-C. and Kushner,S.R. (2010) Single amino acid changes in the predicted RNase H domain of E. coli RNase G lead to the complementation of RNase E mutants. *RNA*, **16**, 1371–1385.

33. Mohanty,B.K. and Kushner,S.R. (2013) Deregulation of poly(A) polymerase I in *Escherichia coli* inhibits protein synthesis and leads to cell death. *Nucleic Acids Res.*, **41**, 1757–1766.

34. Grunberg-Manago, M. (1996) In: Neidhardt,FC, Curtiss,RI, Ingraham,J, Lin,EC, Low,KB, Magasanik,B, Reznikoff,WS, Riley,M, Schaechter,M and Umbarger,HD (eds). *Escherichia coli and Salmonella*. ASM Press, Washington, D.C., **1**, pp. 1432–1457.

35. Kim,M.S., Park,B.H., Kim,S., Lee,Y.J., Chung,J.H. and Lee,Y. (1998) Complementation of the growth defect of an rnpA49 mutant of Escherichia coli by overexpression of arginine tRNA(CCG). *Biochem. Mol. Biol. Int.*, **46**, 1153–1160.

36. Jain,S.K., Gurevitz,M. and Apirion,D. (1982) A small RNA that complements mutants in the RNA processing enzyme ribonuclease P. *J. Mol. Biol.*, **162**, 515–533.

37. Altman,S. (1989) Ribonuclease P: an enzyme with a catalytic RNA subunit. *Adv. Enzymol. Relat. Areas Mol. Biol.*, **62**, 1–36.

38. Moll,I., Leitsch,D., Steinhauser,T. and Blasi,U. (2003) RNA chaperone activity of the Sm-like Hfq protein. *EMBO Rep.*, **4**, 284–289.

39. Altman,S., Baer,M.F., Gold,H., Guerrier-Takada,C., Lawrence,N., Lumelsky,N. and Vioque,A. (1987) In: Inouye,M and Dudock,BS (eds). *Cleavage of RNA by RNase P*. Academic Press, Orlando, pp. 3–15.

40. Hansen,A., Pfeiffer,T., Zuleeg,T., Limmer,S., Ciesiolka,J., Feltens,R. and Hartmann,R.K. (2001) Exploring the minimal substrate requirements for trans-cleavage by RNase P holoenzymes from Escherichia coli and Bacillus subtilis. *Mol. Microbiol.*, **41**, 131–143.

41. Hsieh,P.K., Richards,J., Liu,Q. and Belasco,J.G. (2013) Specificity of RppH-dependent RNA degradation in Bacillus subtilis. *Proc. Natl Acad. Sci. U.S.A.*, **110**, 8864–8869.

42. Zuo,Y. and Deutscher,M.P. (2002) The physiological role of RNase T can be explained by its unusual substrate specificity. *J. Biol. Chem.*, **277**, 29654–29661.

43. Ow,M.C., Perwez,T. and Kushner,S.R. (2003) RNase G of *Escherichia coli* exhibits only limited functional overlap with its essential homologue, RNase E. *Mol. Microbiol.*, **49**, 607–622.

44. Stead,M.B., Marshburn,S., Mohanty,B.K., Mitra,J.P., Ray,C.L.D., Hughes,T. and Kushner,S.R. (2010) Analysis of E. coli RNase E and RNase III activity *in vivo* using tiling microarrays. *Nucleic Acids Res.*, **39**, 3188–3203.

45. Arraiano,C.M., Yancey,S.D. and Kushner,S.R. (1988) Stabilization of discrete mRNA breakdown products in *ams pnp rnb* multiple mutants of *Escherichia coli* K-12. *J. Bacteriol.*, **170**, 4625–4633.

46. Perwez,T. and Kushner,S.R. (2006) RNase Z in *Escherichia coli* plays a significant role in mRNA decay. *Mol. Microbiol.*, **60**, 723–737.

47. Ow,M.C., Liu,Q. and Kushner,S.R. (2000) Analysis of mRNA decay and rRNA processing in *Escherichia coli* in the absence of RNase E-based degradosome assembly. *Mol. Microbiol.*, **38**, 854–866.

48. Li,Z. and Deutscher,M.P. (1994) The role of individual exoribonucleases in processing at the 3' end of *Escherichia coli* tRNA precursors. *J. Biol. Chem.*, **269**, 6064–6071.